Near-Infrared Fluorescence Imaging of Apoptotic Neuronal Cell Death in a Live Animal Model of Prion Disease

Victoria A. Lawson,[†,‡,∥] Cathryn L. Haigh,[†,‡,∥] Blaine Roberts,[‡,#] Vijaya B. Kenche,[†,‡,§] Helen M. J. Klemm,[†] Colin L. Masters,[‡,#] Steven J. Collins,[†,‡] Kevin J. Barnham,[†,§,‡] and Simon C. Drew*[,†,§,‡,⊥]

[†]Department of Pathology, The University of Melbourne, Victoria 3010, Australia, [‡]Mental Health Research Institute, Parkville, Victoria 3052, Australia, [#]Centre for Neuroscience, The University of Melbourne, Victoria 3010, Australia, and [§]The Bio21 Molecular Science and Biotechnology Institute, The University of Melbourne, Victoria 3010, Australia

Abstract

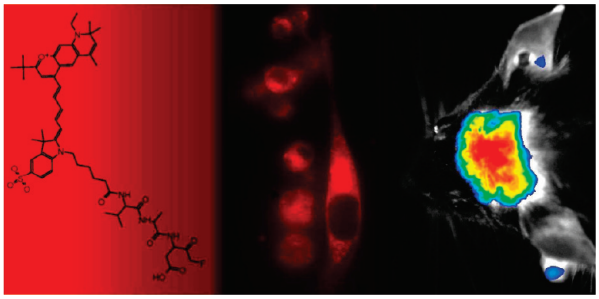

Apoptotic cell death via activation of the caspase family of cysteine proteases is a common feature of many neurodegenerative diseases including Creutzfeldt−Jakob disease. Molecular imaging of cysteine protease activities at the preclinical stage may provide valuable mechanistic information about pathophysiological pathways involved in disease evolution and in response to therapy. In this study, we report synthesis and characterization of a near-infrared (NIR) fluorescent contrast agent capable of noninvasively imaging neuronal apoptosis in vivo, by conjugating a NIR cyanine dye to Val-Ala-Asp-fluoromethylketone (VAD-fmk), a general inhibitor of active caspases. Following intravenous administration of the NIR-VAD-fmk contrast agent, in vivo fluorescence reflectance imaging identified significantly higher levels of active caspases in the brain of mice with advanced but preclinical prion disease, when compared with healthy controls. The contrast agent and related analogues will enable the longitudinal study of disease progression and therapy in animal models of many neurodegenerative conditions.

Keywords: Near infrared, neurodegeneration, prion, mice, apoptosis, caspase, fluorescence, optical imaging

The most common cause of dementia is neurodegeneration arising from the misfolding and aggregation of normal cellular proteins and their deposition, often as amyloid. These neurodegenerative conditions include Alzheimer's disease, Parkinson's disease, Huntington's disease, and transmissible spongiform encephalopathies (prion diseases). Current medical imaging paradigms focus strongly on the detection of amyloid (*1*), but deposition of protein aggregates may arise after significant neuronal dysfunction has occurred (*2*, *3*). Therefore, imaging agents capable of identifying molecular events independent of protein deposition and prior to the onset of clinical symptoms are most desirable.

Fluorescence imaging technology can provide a noninvasive means for disease detection and evaluation of therapeutic strategies in animal models by reporting on the activity of a host of biological events (*4*−*6*). Intrinsic and extrinsic fluorophores that are excited and detected in the visible spectrum have been used extensively for in vitro biological studies employing fluorescence reflectance imaging and microscopy (*4*, *7*). However, their suitability for in vivo imaging applications, including brain imaging, is limited due to the strong attenuation of visible wavelengths by biological tissue (oxy- and deoxyhemoglobin, fat, melanin, water, bone), leading to poor tissue penetration depths (*5*, *8*). Although an optically transparent window chamber can be surgically implanted to slightly improve penetration depth, this requires an invasive craniotomy to be performed. Diseased or dying tissues, especially of the central nervous system, can also exhibit higher levels of autofluorescence in the visible region as compared with healthy tissues, due to the build up of lipofuscin (*9*).

Near-infrared (NIR) wavelengths (650−900 nm) pass more deeply through mammalian tissue and are therefore more suitable for in vivo fluorescence imaging (*6*, *8*). In vivo optical imaging of amyloid plaques in a murine Alzheimer's model has already been demonstrated using various NIR probes (*10*, *11*). However, to monitor disease onset, progression, and response to treatment, contrast agents that are independent of amyloid deposits and sensitive to early markers of disease must be sought. In this study, we present an NIR imaging agent capable of irreversibly binding to active caspases by conjugating a hydrophobic NIR cyanine dye to the broad spectrum

Received Date: July 26, 2010
Accepted Date: September 17, 2010
Published on Web Date: September 30, 2010

DOI: 10.1021/cn100068x | *ACS Chem. Neurosci.* (2010), *1*, 720–727

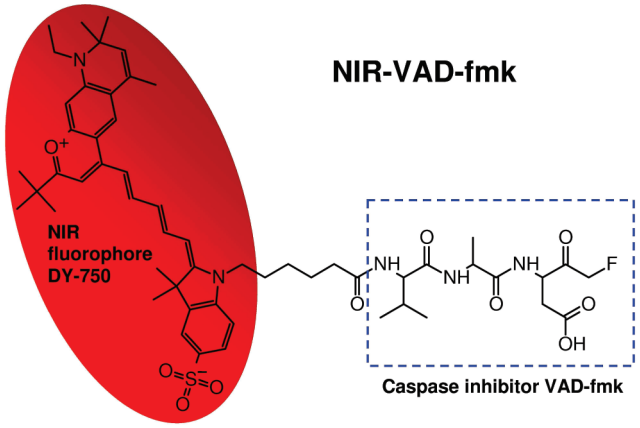

Figure 1. Structure of the contrast agent NIR-VAD-fmk. The fluorophore is a near-infrared cyanine dye (DY-750; Dyomics, GmbH). The VAD-fmk sequence irreversibly binds to the active site of caspase enzymes and is a broad spectrum inhibitor of the caspase family.

caspase inhibitor VAD-fmk (Figure 1). To test the compound in vivo, we assessed its ability to detect neuronal apoptosis in a live murine model of prion disease. Compared with healthy controls, a significant increase in active caspases was measured in the brain of prion-infected mice prior to onset of clinical signs such as ataxia and hind limb paresis. The ability to detect neuronal cell death in living mice prior to development of clinical signs of neurodegenerative disease makes it suitable candidate for screening potential therapeutics targeting early pathogenic pathways.

Methods

Synthesis of a Near-Infrared Fluorescent Inhibitor of Active Caspases

Z-Val-Ala-Asp(OMe)-fmk (Z = benzyloxycarbonyl; fmk = fluoromethylketone) was purchased from SM Biochemicals LLC (Yorba Linda, USA). The peptide was dissolved in a 33% v/v solution of HBr in AcOH (Sigma-Aldrich, Castle Hill, Australia) and stirred for 45 min to form the HBr salt of NH_2-VAD-fmk. The solution was evaporated to dryness and residual HBr/AcOH was removed by washing with ethyl ether, then resuspended in DMF at a concentration of 100 mM. The NIR cyanine dye containing an amino-reactive *N*-hydroxysuccinimidyl-ester (DY-750 NHS-ester, Dyomics GmbH, Germany) was dissolved in DMF and added to the peptide solution at a molar ratio of 1.1:1 in the presence of 3 molar equiv of *N*,*N*-diisopropylethylamine. The reaction was allowed to proceed in the dark overnight at room temperature (RT) with stirring, before the solution was again evaporated to dryness. The labeled product (denoted NIR-VAD-fmk) was purified by RP-HPLC using a Shimadzu LCMS-2010EV LC/MS system with a 5 μm, 2.1 × 150 mm cyano column (Waters Corp., Massachusetts, USA) and a 40−45% MeCN/H_2O gradient in the presence of 0.1% formic acid. Purity was ≥98% as determined from the RP-HPLC trace at 700 nm (Figure S1, Supporting Information). MS analysis indicated the conjugate contained a free aspartyl side chain, indicating loss of the methyl ester during synthesis. $[M + H]^+$: m/z (calc) = 1015.3, m/z (exp) = 1015.0; $[M + Na]^+$: m/z (calc) = 1038.3, m/z (exp) = 1039.0. The ester is not required for cell permeability and is removed by intracellular esterases prior to caspase inhibition. The excitation and emission maxima of NIR-VAD-fmk were comparable to the unconjugated DY-750 ($\lambda_{ex} \approx 740$ nm, $\lambda_{em} \approx 770$ nm). The concentration of purified NIR-VAD-fmk solutions was determined from the optical density at 745 nm using an extinction coefficient of 270 000 M^{-1} cm^{-1}.

Cell Culture

OBL-21 mouse neuronal cells (*12*, *13*) were cultured in Dulbecco's Modified Eagle's Media (DMEM; Gibco − Invitrogen, Victoria, Australia) supplemented with 10% fetal bovine serum (Invitrogen), 50 U mL^{-1} penicillin, and 50 μg mL^{-1} streptomycin solution (Sigma-Aldrich; New South Wales, Australia). All cell lines were maintained at 37 °C with 5% CO_2 in a humidified incubator.

In Vitro Toxicity

Cells were plated to 20% confluency. Five microliters of "one-solution" MTS reagent (Promega, Victoria, Australia) per 100 μL media was added to the media of test and control cultures and incubated under normal culture conditions for 90 min. Reaction product was quantified using absorbance at 462 nm in a Fluostar Optima (BMG Labtech). All results were normalized to cell density.

In Vitro Active Caspase Detection

NIR-VAD-fmk (Figure 1) was solubilized in sterile phosphate buffered saline (PBS) (Gibco − Invitrogen) containing 10% v/v high quality (cell culture tested) sterile-filtered DMSO (Sigma-Aldrich). Cells were incubated with 15 μM NIR-VAD-fmk for 30 min, washed, and imaged under 20× magnification with a Nikon Eclipse TE2000-E epi-fluorescence microscope using an excitation wavelength of 620 ± 30 nm and a 660 nm long-pass filter (Filter set 41008). To correct for background, the average fluorescence intensity of images taken without the addition of fluorescent marker was subtracted in an identical manner from all images.

Mice

All animal procedures conformed to National Health and Medical Research Council of Australia guidelines and were approved by the University of Melbourne Animal Experimentation Ethics Committee. The M1000 prion strain used in this study was derived from the Fukuoka-1 strain of mouse-adapted human prions (*14*). This strain was originally isolated and maintained by passage in Balb/c mice (*15*). Five 6-week old Tga 20 mice were inoculated under methoxyflurane anesthetic in the left parietal region with 30 μL of 1% (w/v) homogenate prepared in PBS from a pool of brains derived from Balb/c mice with clinical prion disease induced by M1000 infection. The Tga20 transgenic mouse line overexpresses murine PrP^C and mice develop signs of clinical prion disease (bradykinesis, kyphosis, ataxia, and hind limb paresis) approximately 60 days after an intracerebral prion inoculation, with terminal disease occurring within days of symptom onset (*16*). Three 5-week old Tga20 mice received an intracerebral prion inoculation with 30 μL of 1% w/v brain homogenate prepared from uninfected Balb/c mice and served as age matched, sham inoculated controls.

DOI: 10.1021/cn100068x | *ACS Chem. Neurosci.* (2010), *1*, 720–727

In Vivo Toxicity

NIR-VAD-fmk (Figure 1) was prepared in sterile phosphate buffered saline (PBS) (Gibco − Invitrogen) containing 10% v/v high quality (cell culture tested) sterile-filtered DMSO (Sigma-Aldrich). To screen for possible toxicity of the new compound, two healthy 5-week-old Tga20 mice were administered a 100 μL injection of a 0.5 mM NIR-VAD-fmk solution via the lateral tail vein. They were monitored for 2 h immediately following treatment, and thereafter daily for 1 week, whereupon a second dose was administered.

In Vivo Active Caspase Detection

Fifty-four days after inoculation, three prion-infected (I1, I2, I3) and three sham-inoculated Tga20 mice (U1, U2, U3) were administered 200 μL of a 0.25 mM NIR-VAD-fmk solution via the lateral tail vein. To assess possible contributions from nonspecific autofluorescence of diseased tissue, an additional two prion-infected Tga20 mice (I4, I5) received 200 μL of inactive PBS/DMSO diluent only. PBS was used in preference to a NIR labeled version of the well-known inactive substrate FA-fmk. Although inactive against caspases, FA-fmk inhibits cathepsins (*17*), whose activities are up-regulated in prion-infected mouse neuronal N2a cells (*18*). Moreover, it is not possible to predict whether a fluorescent NIR-FA-fmk analogue will exhibit blood-brain-barrier permeability comparable with NIR-VAD-fmk. Prior to imaging, NIR-VAD-fmk was permitted to circulate for 30 min following injection to allow circulation and excretion of any unbound probe. Mice were subsequently anaesthetised by the intraperitoneal administration of ketamine (80 mg kg^{-1})/xylazine (10 mg kg^{-1}) and their heads shaved in preparation for fluorescence reflectance imaging.

Anesthetized mice were transferred to the dark box of a LAS-3000 imaging system (FujiFilm, Japan). Fluorescence reflectance images (16 bit, 36.7 × 36.7 μm pixel size) were obtained using a 710 nm LED epi-illuminator and a 785 nm long-pass filter with an exposure time of 5 s and an aperture of F0.85. These were superimposed upon monochrome images obtained using a white epi-illuminator with an exposure time of 16.7 ms and an aperture of F2.8. Image analysis was performed using Multi Gauge V3.0 software (FujiFilm, Japan). Statistical analyses were carried out using Minitab 15.1.30.0 statistical software.

At the conclusion of imaging anaesthetized mice were euthanised by cardiac perfusion with PBS and brains sectioned through the sagittal plane. One half was snap frozen in liquid nitrogen and stored at −80 °C and the other half fixed in 10% neutral buffered formalin (NBF).

Western Blotting

Brain homogenates (20% w/v) were prepared in PBS using a FastPrep Homogenizer (ThermoSavant) using a single cycle of homogenization before being further diluted to 6% (w/v) in PBS and final concentration of 0.1% SDS (to aid digestion of PrP^C) and treated with proteinase K (100 μg mL^{-1}, 1 h, 37 °C). PK-digestion was stopped by the addition of PefaBloc SC (Roche; 4 mM) and 4 × LDS loading dye (containing 12% v/v beta-mercaptoethanol) and heated to 100 °C for 10 min. Samples were electrophoresed on a 12% (bis/tris) gel (NuPAGE Invitrogen) at 200 V for 50 min in MES electrophoresis buffer (Invitrogen) and transferred to a PVDF membrane at 85 V for 60 min in Tris/glycine transfer buffer (25 mM Tris, 200 mM glycine, 20% methanol). Blots were blocked in 5% skim milk powder in PBS/0.1% Tween-20 (PBST) for 1 h at room temperature (RT) and probed for 1 h at RT with rabbit polyclonal antibody 03R19 raised to residues 89−103 of mouse PrP (*19*). The blot was washed at RT 1 × 10 min, and 3 × 3 min, probed with antirabbit-HRP for 1 h at RT, washed as described, and developed using ECL-plus (GE Healthcare). The prepared membrane was imaged using the LAS-3000 imaging system and analysis was performed using Multi Gauge V3.0 software (FujiFilm, Japan). Following normalization for total protein (BCA; Pierce) homogenates prepared from U1-3 and I1-3 containing 50 μg of total protein were electrophoresed as described above and probed overnight at 4 °C with an antibody to cleaved caspase-3 (Asp175) (cat. no. 9661; Cell signaling Technology), washed, incubated with antirabbit HRP for 1 h at RT, washed and developed with ECL-advance (GE Healthcare) before imaging and analysis as described above. Statistical analyses were carried out using Minitab 15.1.30.0 statistical software.

Immunohistochemistry

Brain hemispheres fixed in 10% NBF were immersed in 99% formic acid for 1 h prior to routine processing and immunostaining. Half-brains were paraffin embedded and 7 μm sections cut and mounted on glass slides (Superfrost plus; Thermo). Sections were deparaffinized and rehydrated through a graded ethanol series to deionized water and stained with hematoxylin and eosin or immunostained with ICSM18 anti-PrP monoclonal antibody (D-Gen Ltd., London, UK) (*20*). For immunostaining, rehydrated sections were autoclaved for 20 min at 132 °C and once cooled, washed in deionized water, exposed to 4 M guanidine thiocyanate for 2 h at 4 °C, washed and treated with 96% formic acid for 5 min. After blocking with 20% fetal bovine serum for 30 min, sections were incubated with ICSM18 overnight at 4 °C. Sections were then processed using a avidin−biotin immunohistochemical process (LSAB+; Dako) and developed using diaminobenzadine (DAB+; DAKO) and counterstained with hematoxylin.

Results and Discussion

The ability of labeled VAD-fmk compounds to detect active caspases is well characterized (*21*), and their specificity for labeling apoptotic neuronal cells in live mice has been clearly established (*3*). Nevertheless, prior to testing the new NIR-VAD-fmk contrast agent in vivo, we first examined its toxicity and cell permeability in vitro using a mouse neuronal (OBL-21) cell line. No significant reduction in cell viability (measured by MTS reduction) was seen in response to treatments ranging in concentration by 4 orders of magnitude, even after 3 days' constant exposure to 75 μM. (This exceeds the nominal NIR-VAD-fmk blood concentration of 55.5 μM in mice, based upon a typical blood volume of 800 μL and a 200 μL injection of 0.25 mM NIR-VAD-fmk.) NIR-VAD-fmk (Figure S2, Supporting Information). To assess the cell permeability and the specificity of the NIR-VAD-fmk binding in response to apoptotic stimulus, the compound was applied to the OBL-21 mouse neuronal cells following 10 min

DOI: 10.1021/cn100068x | ACS Chem. Neurosci. (2010), 1, 720–727

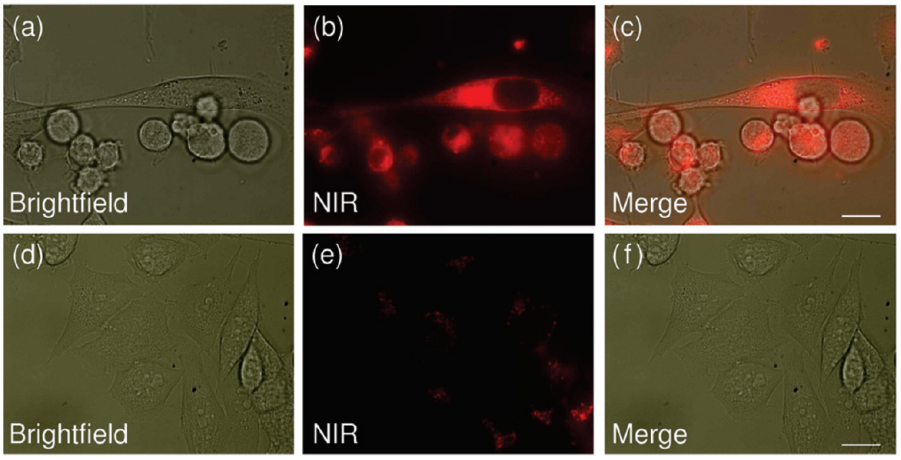

Figure 2. NIR-VAD-fmk localization of caspase activation in OBL-21 mouse neuronal cells (a−c) 24 h post exposure to 10 min UV irradiation. (d−f) untreated control. After 24 h, cells were incubated with 15 μM NIR-VAD-fmk for 30 min, washed and imaged by fluorescence microscopy at 60× magnification. Scale bar = 20 μm.

ultraviolet (UV) irradiation. UV exposure initiates apoptosis via an intrinsic cell death pathway involving mitchondrial release of cytochrome c, activation of the initiator caspase 9 and subsequent activation effector caspases 3 and 6 (*22*). In comparison with the nonirradiated control, the UV irradiated cells displayed strong intracellular NIR fluorescence (Figure 2), demonstrating the cell-permeability of NIR-VAD-fmk and its ability to bind to active caspases. Binding of the probe could be observed within hours of UV insult (Figure S3, Supporting Information), and at 24 h a large number of cells could be demarcated by NIR-VAD-fmk binding (Figure S4, Supporting Information). Untreated OBL-21 cells showed only a low level of intracellular binding, consistent with basal levels of active caspases associated with normal cellular processes, such as cell division and differentiation (*23*).

Having established that NIR-VAD-fmk was nontoxic and able to permeate and bind to active caspases in cultured cells, we examined its ability to label active caspases in live animals using a murine model of prion disease. In healthy controls, no signs of toxicity or adverse reaction was observed following administration of a single dose of NIR-VAD-fmk, nor after a second dose one week later. NIR-VAD-fmk was then administered to Tga20 mice 54 days post inoculation with M1000 prions or a sham inoculation (Figure 3). At this time there was no evidence of weight loss or overt signs of clinical prion disease, which occurs approximately 60 days post inoculation in this transgenic mouse line. Nevertheless, quantification of NIR-VAD-fmk binding by fluorescence reflectance imaging revealed increased levels of active caspases in the brains of prion-infected mice compared with mice that received an intracerebral inoculation with uninfected brain homogenate (Figure 4). Prion-infected mice that received only the DMSO/PBS vehicle instead of NIR-VAD-fmk yielded a negligible autofluorescent signal (Figure S5, Supporting Information), indicating that the increased fluorescence was not attributable to accumulation of lipofuscin in prion disease (*9*).

Following imaging, animals were euthanized and the brain pathology was examined using traditional markers of disease neuropathology. Consistent with the in vivo observation of NIR-VAD-fmk fluorescence in prion-infected mice, Western immunoblot analysis showed a significant increase in cleaved caspase-3 (a central effector caspase) in prion-infected mice (Figure 5). Western immunoblot analysis confirmed the presence of PrP^{Sc} in prion infected mice and absence in sham-inoculated controls (Figure 6a). Hematoxylin and eosin staining was consistent with the preclinical state of the animals with little to no vacuolation apparent in the hippocampus, thalamus, pons or occipital cortex of infected mice I1, I2, and I3 that received NIR-VAD-fmk and mild to moderate vacuolation in infected mice I4 and I5 that by chance received the vehicle (Figure 6b). PrP^{Sc} deposition was similarly mild or undetectable in all prion infected mice (Figure 6).

In hippocampal CA2 neurons, apoptosis has been shown to occur prior to the accumulation of PrP^{Sc} and the onset of clinical disease in a mouse-passaged 87 V scrapie strain (*2*). However, confirmation of apoptosis required culling the mice to carry out terminal deoxynucleotidyl transferase-mediated uridine triphosphate nick end labeling (TUNEL) staining to show DNA fragmentation within the brain. In this study, we have noninvasively measured caspase activation associated with apoptotic neuronal cell death in live prion-infected mice 54 days postinoculation prior to development of disease (*16*). NIR imaging of molecular processes such as caspase and other protease activities at the preclinical stage promises to provide more valuable mechanistic

DOI: 10.1021/cn100068x | *ACS Chem. Neurosci.* (2010), *1*, 720–727

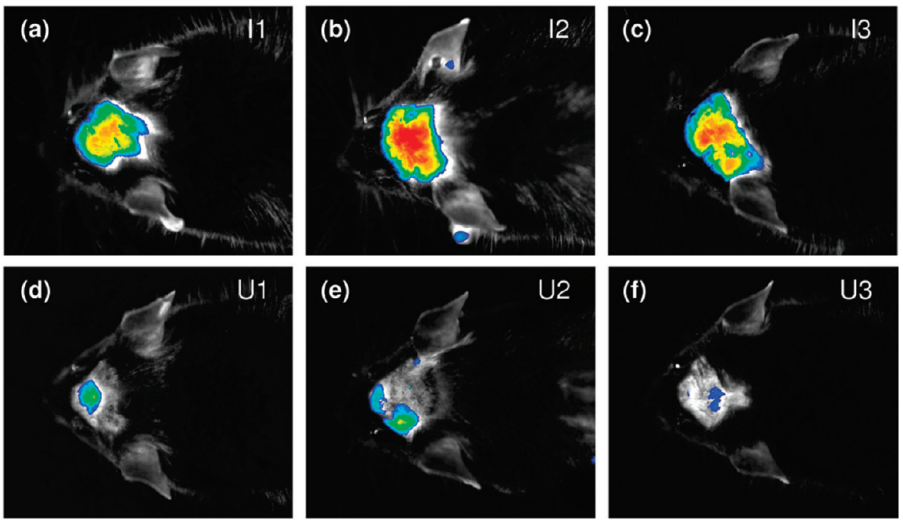

Figure 3. Overlay of in vivo fluorescence and white-light images of (a−c) prion-infected (I1−I3) and (d−f) sham inoculated (U1−U3) Tga20 mice, following administration of a NIR-VAD-fmk dose, 54 days postinoculation.

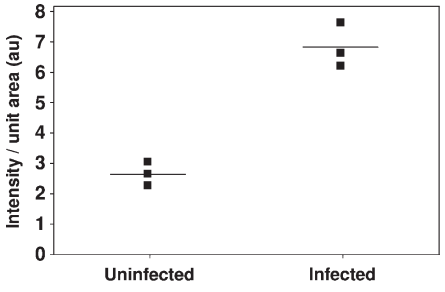

Figure 4. Quantification of the images shown in Figure 3. Prion-infected mice that received the NIR-VAD-fmk exhibited a significantly higher fluorescence emission compared with the sham-inoculated healthy (uninfected) controls (Mann−Whitney, one-tailed, $W = 15.0$, $p = 0.040$, $n = 3$). Black squares represent the average fluorescence intensity per unit area of each NIR image. Horizontal bars denote the group means.

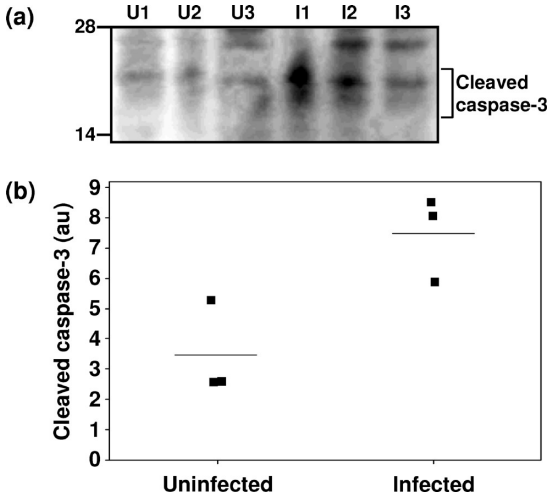

Figure 5. (a) Western immunoblot analysis of brain homogenates from prion-infected (I1−I3) and sham-inoculated (uninfected) (U1−U3) mice administered NIR-VAD-fmk. Molecular weight markers are shown. Consistent with in vivo imaging, quantification of immunoreactivity against cleaved caspase-3 (b) indicated increased levels in prion-infected mice (Mann−Whitney, one-tailed, $W = 15.0$, $p = 0.040$, $n = 3$). Horizontal bars denote the group means.

information about pathophysiological pathways involved in neurodegeneration compared with diagnostic imaging modalities that focus on detection of late-stage markers of disease such as amyloid formation.

A number of other NIR contrast agents for detecting cell death have been developed in recent years. For example, a NIR (Cy5.5) fluorophore has been conjugated to annexin-V to detect externalization of phosphatidylserine at the cell membrane during tumor apoptosis (*24*). NIR-VAD-fmk is demonstrably blood-brain-barrier permeable making it suitable for brain imaging applications and can be further refined to detect specific caspases by changing the caspase recognition sequence. Analogous NIR compounds based upon caspase substrates rather than inhibitors have also been developed. One example is the enzyme-activatable Cy5.5-DEVD substrate tethered to cell-permeable nanoparticles, which has been shown to detect active caspases 3 and 7 in cell culture (*25*). Another involves intracellular delivery of DEVD conjugated to Alexa Fluor 647 and QSY 21 dyes via a cell-penetrating KKKRKV peptide sequence, which was demonstrated to detect NMDA-induced apoptosis of retinal ganglion cells following intravitreal injection in live rats (*26*). However, the blood-brain-barrier permeability of such compounds for brain imaging applications remains unknown. Moreover, such compounds do not bind irreversibly to active caspases and therefore must rely on self-quenching until the substrate is cleaved. Depending upon disease pathophysiology, the kinetics of uptake of the uncleaved (nonfluorescent) substrate and clearance of the cleaved (fluorescent) substrate may vary between healthy and diseased individuals,

DOI: 10.1021/cn100068x | *ACS Chem. Neurosci.* (2010), *1*, 720–727

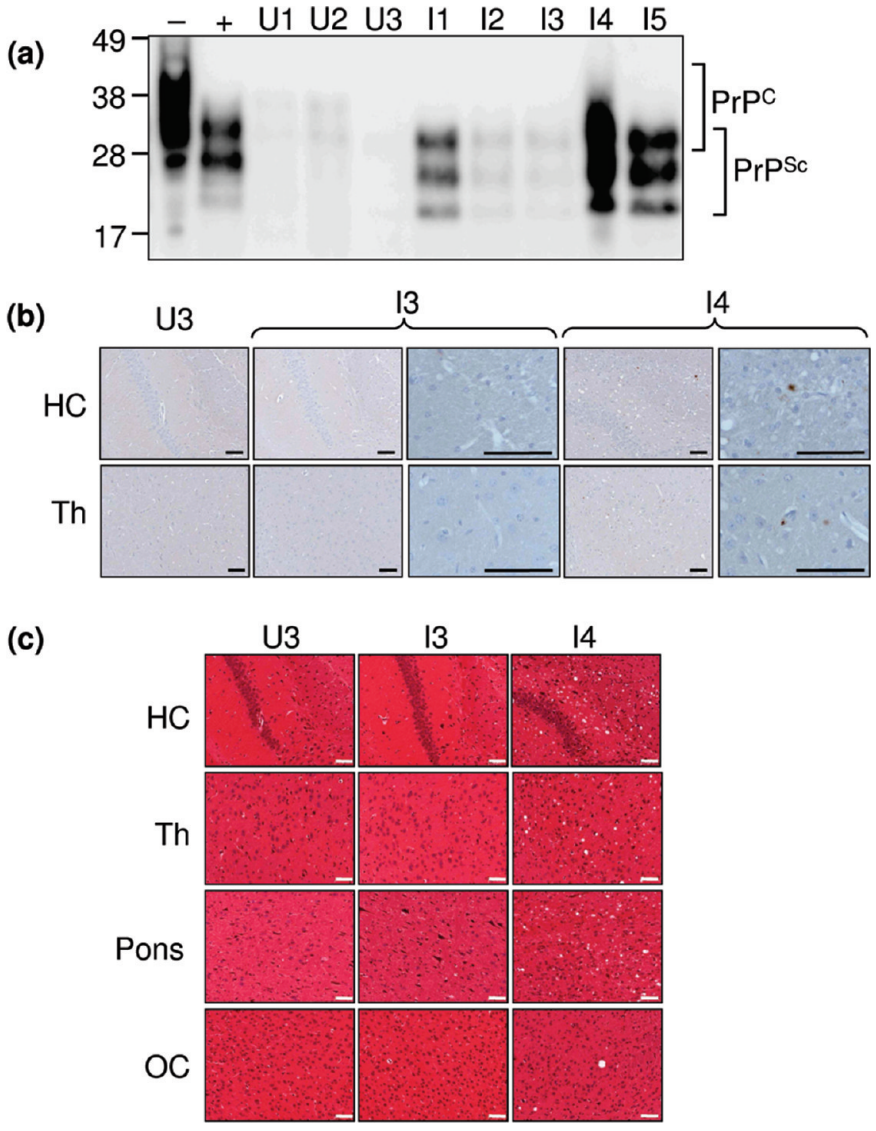

Figure 6. Pathology associated with prion-infected Tga20 mice. (a) PK-treated (100 μg mL^{-1}, 1 h, 37 °C) homogenates prepared from sham inoculated (U1−U3) and prion-infected (I1−I5) Tga20 mice were Western immunoblotted with 03R19. Homogenates prepared from a Tga20 mouse with clinical disease are shown before (−) and after (+) PK treatment for comparison. Molecular weight markers (kDa) are shown. (b) Immunostaining of PrP^{Sc} using ICSM18 and (c) hematoxylin and eosin staining of sham inoculated (U3) or prion infected mice with low PrP^{Sc} (I3) and high PrP^{Sc} (I4) load. Images show the CA1 region of the hippocampus (HC), thalamus (Th), Pons and occipital cortex (OC). Images were taken at ×20 and ×40 magnification. Scale bars shown are 50 μm.

making it difficult to compare relative concentrations measured at the time of imaging. The use of the NIR-VAD-fmk caspase inhibitor, rather than a substrate, can eliminate this potential complication since binding is irreversible (covalent); hence, in both healthy and diseased mice, one only requires that sufficient time be given for the probe to circulate and for unbound probe to be excreted. As proof of principle, we have quantified the degree of binding of a broad spectrum caspase inhibitor in vivo using a relatively inexpensive fluorescence reflectance imaging system. However, the procedure employed herein can be extended to include inhibitors of specific caspases across the spectrum of neurodegenerative diseases by varying the target peptide sequence (*21*), while additional improvements in depth resolution and spatial localization may be achieved using a fluorescence tomographic imaging approach (*6*, *8*, *27*).

Conclusions

A range of evidence supports an apoptotic cell death mechanism in animal and human forms of prion disease, including Creutzfeldt−Jakob Disease (*2*, *28*−*34*). However, to the best of our knowledge, there have been no demonstrations of noninvasive detection of neuronal apoptosis associated with such neurodegeneration in vivo. While it is possible to perform in vivo labeling by

DOI: 10.1021/cn100068x | *ACS Chem. Neurosci.* (2010), *1*, 720–727

administering green and red fluorescent VAD-fmk compounds to live animals, quantifying the degree of caspase activation at the time of labeling requires either fluorescence imaging of the brain to be examined ex vivo or for an invasive window chamber to be surgically inserted in the skull (*3*). In this study, we have synthesized and validated a nontoxic cell and blood-brain-barrier permeable NIR probe capable of demarcating brain cells with active caspases in vivo.

The NIR-VAD-fmk compound was shown to permeate cultured neuronal cells and bind to caspases activated in response to an apoptotic stimulus, with the signal easily distinguishable from low basal levels of active caspases as part of normal cell function. The contrast agent showed no toxicity to cultured OBL-21 mouse neuronal cells and subsequently to live mice over a period of two weeks, following two evenly spaced doses equivalent to that used for imaging. In vivo, NIR-VAD-fmk was able to detect a significant brain elevation of active caspases in an animal model of prion disease prior to onset of clinical features. The ability to progressively monitor neuronal loss in individual mice in vivo will permit longitudinal studies to assess the preclinical efficacy of therapeutic candidates and identify the underlying molecular mechanisms of neurodegeneration.

Supporting Information Available

LC/MS characterization, excitation/emission spectra, cell viability data, widefield fluorescence microscopy data, in vivo fluorescence reflectance images.This material is available free of charge via the Internet at http://pubs.acs.org.

Author Information

Corresponding Author

[*] To whom correspondence should be addressed. E-mail: drew@mpi-muelheim.mpg.de.

Present Addresses

[⊥] Current address: Max Planck Institut für Bioanorganische Chemie, 45470 Mülheim an der Ruhr, Germany.

Author Contributions

[‖] These authors contributed equally to this work. V.A.L. performed in vivo experiments, tissue preparation, IHC, western blotting and data analysis. C.L.H. performed cell culture, in vitro toxicity and caspase detection, fluorescence microscopy and data analysis. B.R. performed purification. V.B.K. performed chemical synthesis. H.M.J.K. assisted with in vivo experiments and tissue preparation. C.L.M. provided intellectual guidance and manuscript review. S.J.C. analyzed the data and assisted with manuscript review. K.J.B. analyzed the data and assisted with manuscript review. S.C.D. conceived the project, performed chemical synthesis and purification, fluorescence reflectance imaging and data analysis, and wrote the manuscript with input from V.A.L. and C.L.H.

Funding Sources

This project was funded by a grant from VCF - George Perry Fund, The Arthur and Mary Osborn Charitable Trust, and the William Buckland Foundation, which is managed by ANZ Trustees. V.A.L. was supported by a CR Roper fellowship (The University of Melbourne). S.J.C. was supported by an NHMRC Practitioner Fellowship #400183.

Acknowledgment

Tga20 mice bred for this study originated from a generous gift from Prof. Charles Weissmann, The Scripps Research Institute, La Jolla, California, USA. The OBL21 cell line used in this study was a kind gift from Dr. Michael Oldstone, The Scripps Research Institute, La Jolla, California, USA.

References

1. Nordberg, A., Rinne, J. O., Kadir, A., and Langström, B. (2010) *Nat. Rev. Neurol. 6*, 78–87.

2. Jamieson, E., Jeffrey, M., Ironside, J., and Fraser, J. (2001) *Neuroreport 12*, 2147–2153.

3. de Calignon, A., Fox, L., Pitstick, R., Carlson, G., Bacskai, B., Spires-Jones, T., and Hyman, B. (2010) *Nature 464*, 1201–1204.

4. Tung, C.-H. (2004) *Biopolymers* (*Pept. Sci.*) *76*, 391–403.

5. Mahmood, U., and Weissleder, R. (2003) *Mol. Cancer Ther. 2*, 489–496.

6. Weissleder, R., and Pittet, M. (2008) *J. Pathol. 452*, 580–589.

7. Chudakov, D. M., Lukyanov, S., and Lukyanov, K. A. (2005) *Trends Biotechnol. 23*, 605–613.

8. Hawrysz, D., and Sevick-Muraca, E. (2000) *Neoplasia 2*, 388–417.

9. Boellaard, J., Schlote, W., and Tateishi, J. (1989) *Acta Neuropathol. 78*, 410–418.

10. Raymond, S., Skoch, J., Hills, I., Nesterov, E., Swager, T., and Bacskai, B. (2008) *Eur. J. Nucl. Med. Mol. Imaging 35* (Suppl 1), S93–S98.

11. Ran, C., Xu, X., Raymond, S., Ferrara, B., Neal, K., Bacskai, B., Medarova, Z., and Moore, A. (2009) *J. Am. Chem. Soc. 131*, 15257–15261.

12. Chesebro, B., Wehrly, K., Caughey, B., Nishio, J., Ernst, D., and R., R. (1993) *Dev. Biol. Stand. 80*, 131–140.

13. Ryder, E., Snyder, E., and Cepko, C. (1990) *J. Neurobiol. 21*, 356–375.

14. Tateishi, J., Ohta, M., Koga, M., Sato, Y., and Kuroiwa, Y. (1979) *Ann. Neurol. 5*, 581–584.

15. Brazier, M. W., Lewis, V., Ciccotosto, G. D., Klug, G. M., Lawson, V. A., Cappai, R., Ironside, J. W., Masters, C. L., Hill, A. F., White, A. R., and Collins, S. J. (2006) *Brain Res. Bull. 68*, 346–354.

16. Fischer, M., Rulicke, T., Raeber, A., Sailer, A., Moser, M., Oesch, B., Brandner, S., Aguzzi, A., and Weissmann, C. (1996) *EMBO J. 15*, 1255–1264.

17. Faubion, W., Guicciardi, M., Miyoshi, H., Bronk, S., Roberts, P., Svingen, P., Kaufmann, S., and Gores, G. (1999) *J. Clin. Invest. 103*, 137–145.

18. Zhang, Y., Spiess, E., Groschup, M., and Bürkle, A. (2003) *J. Gen. Virol. 84*, 2279–2283.

DOI: 10.1021/cn100068x | *ACS Chem. Neurosci.* (2010), *1*, 720–727

19. Lawson, V. A., Vella, L. J., Stewart, J. D., Sharples, R. A., Klemm, H., Machalek, D. M., Masters, C. L., Cappai, R., Collins, S. J., and Hill, A. F. (2008) *Int. J. Biochem. Cell Biol. 40*, 2793–2801.

20. White, A., Enever, P., Tayebi, M., Mushens, R., Linehan, J., Brandner, S., Anstee, D., Collinge, J., and Hawke, S. (2003) *Nature 422*, 80–83.

21. Chan, S., and Mattson, M. (1999) *J. Neurosci. Res. 58*, 167–190.

22. Kulms, D., and Schwarz, T. (2002) *Skin Pharmacol. Appl. Skin Physiol. 15*, 342–347.

23. Nhan, T., Liles, W., and Schwartz, S. (2006) *Am. J. Path. 169*, 729–737.

24. Petrovsky, A., Schellenberger, E., Josephson, L., Weissleder, R., and Bogdanov, A. (2003) *Cancer Res. 63*, 1936–1942.

25. Kim, K., Lee, M., Park, H., Kim, J.-H., Kim, S., Chung, K., Choi, H., Kim, I.-S., Seong, B., and Kwon, I. (2006) *J. Am. Chem. Soc. 128*, 3490–3491.

26. Maxwell, D., Chang, Q., Zhang, X., Barnett, E., and Piwnica-Worms, D. (2010) *Bioconjugate Chem. 20*, 702–709.

27. Graves, E., Weissleder, R, and Ntziachristos, V. (2004) *Curr. Mol. Med. 4*, 419–430.

28. Lucassen, P., Williams, A., Chung, W., and H., F. (1995) *Neurosci. Lett. 198*, 185–188.

29. Giese, A., Groschup, M., Hess, B., and Kretzschmar, H. (1995) *Brain Path. 5*, 213–221.

30. Puig, B., and Ferrer, I. (2001) *Acta Neuropathol. 102*, 207–215.

31. Jesionek-Kupnicka, D., Kordek, R., Buczyski, J., and Liberski, P. (2001) *Acta Neurobiol. 61*, 13–19.

32. Hetz, C., Russelakis-Carneiro, M., Maundrell, K., Castilla, J., and Soto, C. (2003) *EMBO J. 22*, 5435–5445.

33. Liberski, P., Sikorska, B., Bratosiewicz-Wasik, J., Gajdusek, D., and Brown, P. (2004) *Int. J. Biochem. Cell Biol. 36*, 2473–2490.

34. Hetz, C., Russelakis-Carneiro, M., Wälchli, S., Carboni, S., Vial-Knecht, E., Maundrell, K., Castilla, J., and Soto, C. (2005) *J. Neurosci. 25*, 2793–2802.

DOI: 10.1021/cn100068x | *ACS Chem. Neurosci.* (2010), *1*, 720–727